Synthesis, Characterization, Langmuir−Blodgett Film-Forming Property, and Second-Order Nonlinear Optical Study of Rhenium(I) and Ruthenium(II) Diimine Complexes

Jiaxin Zhang, Ben Wai-Kin Chu,* Nianyong Zhu, and Vivian Wing-Wah Yam*

Department of Chemistry and HKU-CAS Joint Laboratory on New Materials, The University of Hong Kong, Pokfulam Road, Hong Kong, People's Republic of China

Received January 12, 2007

A series of rhenium(I) and ruthenium(II) complexes of general formulas *fac*-[Re(CO)$_3$ClL] and [Ru(bpy)$_2$L](PF$_6$)$_2$ (L = *N*-(4-biphenyl)pyridine-2-carbaldimine (**L1**), *N*-[4-(4′-octadecyloxy)biphenyl]pyridine-2-carbaldimine (**L2**), (5-octadecyloxy)-2-pyridine-*N*-(4-biphenyl)carbaldimine (**L3**), and (5-octadecyloxy)-2-pyridine-*N*-[4-(4′-octadecyloxy)biphenyl]carbaldimine (**L4**)) were synthesized and characterized, and their photophysical properties were also studied. The X-ray crystal structures of *fac*-[Re(CO)$_3$ClL1] and [Ru(bpy)$_2$L1](PF$_6$)$_2$ have been determined. These complexes were capable of forming stable Langmuir−Blodgett (LB) films, as revealed by the study of their surface pressure−area (π−*A*) isotherms, and their second-harmonic generation (SHG) properties were also investigated.

Introduction

The search for new molecular materials with large second-order nonlinear optical (NLO) properties is of great current interest due to their potential applications in novel optoelectronic and photonic technologies.[1] Among these studies, transition metal complexes represent an emerging and growing class of materials.[2−5] Compared to organic molecules, metal complexes possess low-lying charge-transfer states, which can be associated with large nonlinearities.[4,6] They also offer a larger variety of structures and a diversity of electronic properties tunable by virtue of the coordinated metal center.[7] Second-harmonic generation (SHG) effects are usually observed only from noncentrosymmetric materials. The Langmuir−Blodgett (LB) technique, which is recognized as being important for controlling the structure at the molecular level, is among one of the best means of preparing SHG-active materials,[8] since noncentrosymmetric alignment of molecules can be achieved at monolayer levels.

Rhenium(I) tricarbonyl diimine and ruthenium(II) bipyridyl complexes with low-lying metal-to-ligand charge-transfer excited states have received enormous attention due to their potential uses as luminescent sensors[9] and photosensitizers[10] in photoinduced electron-transfer and energy-transfer reactions. Recently, the second-order NLO properties of several rhenium(I)[11] and ruthenium(II)[12] complexes incorporated into LB films were reported by us and others. To further extend the work, in this paper, we describe the synthesis, characterization, and LB film studies of a series of new rhenium(I) tricarbonyl diimine and ruthenium(II) bipyridyl complexes, and two of the complexes were found to display second-order NLO properties in LB films.

(1) (a) Prasad, P. N.; Williams, D. J. *Introduction to Nonlinear Optical Effects in Molecules and Polymers*; Wiley: New York, 1991. (b) *Molecular Nonlinear Optics: Materials, Physics and Devices*; Zyss, J., Ed.; Academic Press: Boston, 1994. (c) *Materials for Nonlinear Optics, Chemical Perspectives*; Marder, S. R., Sohn, J. E., Stucky, G. D., Eds.; ACS Symposium Series 455, Washington DC, 1991. (d) *Nonlinear Optics of Organic Molecules and Polymers*; Nalwa, H. S., Miyata, S., Eds.; CRC Press: Boca Raton, FL, 1997.

(2) Nalwa, H. S. *Appl. Organomet. Chem.* **1991**, *5*, 349.

(3) Marder, S. R. In *Inorganic Materials*; Bruce, D. W., O'Hare, D., Eds.; Wiley: New York, 1992.

(4) (a) Long, N. J. *Angew. Chem., Int. Ed. Engl.* **1995**, *34*, 21. (b) Le Bozec, H.; Renouard, T. *Eur. J. Inorg. Chem.* **2000**, 229.

(5) Whittall, I. R.; McDonagh, A. M.; Humphrey, M. G.; Samoc, M. *Adv. Organomet. Chem.* **1998**, *42*, 291.

(6) (a) Kanis, D. R.; Lacroix, P. G.; Ratner, M. A.; Marks, T. J. *J. Am. Chem. Soc.* **1994**, *116*, 10089. (b) Lacroix, P. G. *Eur. J. Inorg. Chem.* **2001**, 339.

(7) (a) Di Bella, S.; Fragalà, I.; Ledoux, I.; Marks, T. J. *J. Am. Chem. Soc.* **1995**, *117*, 9481. (b) Di Bella, S.; Fragalà, I.; Marks, T. J.; Ratner, M. A. *J. Am. Chem. Soc.* **1996**, *118*, 12747. (c) Di Bella, S.; Fragalà, I.; Ledoux, I.; Diaz-Garcia, M. A.; Marks, T. J. *J. Am. Chem. Soc.* **1997**, *119*, 9550. (d) Di Bella, S. *Chem. Soc. Rev.* **2001**, *30*, 355. (e) Coe, B. J. In *Comprehensive Coordination Chemistry II*; McCleverty, J. A., Meyer, T. J., Eds.; Elsevier Pergamon: Oxford, U.K., 2004; Vol. 9, pp 621−687. (f) Maury, O.; Le Bozec, H. *Acc. Chem. Res.* **2005**, *38*, 691. (g) Cariati, E; Pizzotti, M.; Roberto, D.; Tessore, F.; Ugo, R. *Chem. Soc. Rev.* **2006**, *250*, 1210. (h) Coe, B. J. *Acc. Chem. Res.* **2006**, *39*, 383.

(8) (a) Blodgett, K.; Langmuir, I. *J. Phys. Rev.* **1937**, *51*, 964. (b) Ulman, A. *An Introduction to Ultrathin Organic Films: From Langmuir-Blodgett to Self-Assembly*; Academic Press: Boston, 1991.

(9) (a) Yam, V. W. W.; Wong, K. M. C.; Lee, V. W. M.; Cheung, K. K. *Organometallics* **1995**, *14*, 4034. (b) Sacksteder, L.; Lee, M.; Demas, J. N. *J. Am. Chem. Soc.* **1993**, *115*, 8230. (c) Yoon, D. I.; Berg-Brennan, C. A.; Lu, H.; Hupp, J. T. *Inorg. Chem.* **1992**, *31*, 3192. (d) Berg-Brennan, C. A.; Yoon, D. I.; Hupp, J. T. *Inorg. Chem.* **1996**, *35*, 2032.

(10) (a) Balzani, V.; Bolleta, F.; Gandolfi, M. T.; Maestri, M. *Top. Curr. Chem.* **1978**, *75*, 1. (b) Sutin, N.; Creutz, C. *Pure Appl. Chem.* **1980**, *52*, 2717. (c) Sutin, N. *J. Photochem.* **1979**, *10*, 19. (d) Kalyanasundaram, K. *Coord. Chem. Rev.* **1982**, *46*, 159. (e) Vlcek, A., Jr. *Coord. Chem. Rev.* **2000**, *200−202*, 933. (f) Bignozzi, C. A.; Argazzi, R.; Kleverlaan, C. *J. Chem. Soc. Rev.* **2000**, *29*, 87. (g) Sun, L.; Hammarström, L.; Åkermark, B; Styring, S. *Chem Soc. Rev.* **2001**, *30*, 36. (h) Dürr, H.; Bossmann, S. *Acc. Chem. Res.* **2001**, *34*, 905. (i) Huynh, M. H. V.; Dattelbaum, D. M.; Meyer, T. J. *Coord. Chem. Rev.* **2005**, *249*, 457. (j) Alstrum-Acevedo, J. H.; Brennaman, M. K.; Meyer, T. J. *Inorg. Chem.* **2005**, *44*, 6802.

(11) (a) Yam, V. W. W.; Lau, V. C. Y.; Wang, K. Z.; Cheung, K. K.; Huang, C. H. *J. Mater. Chem.* **1998**, *8*, 89. (b) Yam, V. W. W.; Wang, K. Z.; Wang, C. R.; Yang, Y.; Cheung, K. K. *Organometallics* **1998**, *17*, 2440. (c) Yam, V. W. W.; Yang, Y.; Yang, H. P.; Cheung, K. K. *Organometallics* **1999**, *18*, 5252.

(12) (a) Sakaguchi, H.; Nakamura, H.; Nagamura, T.; Ogawa, T.; Matsuo, T. *Chem. Lett.* **1989**, 1715. (b) Nagamura, T.; Sakaguchi, H. *Thin Solid Films* **1992**, *210−211*, 162. (c) Yamada, S.; Nakano, T.; Matsuo, T. *Thin Solid Films* **1994**, *245*, 196. (d) Chu, B. W. K.; Yam, V. W. W. *Inorg. Chem.* **2001**, *40*, 3324.

10.1021/om070030b CCC: $37.00
Publication on Web 09/28/2007

Scheme 1. Structures of the Ligands and Their Re(I) and Ru(II) Complexes

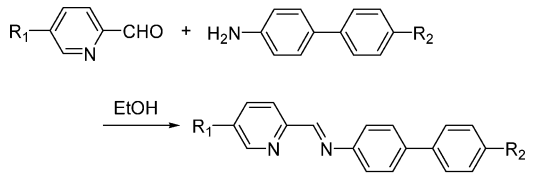

L1, $R_1 = R_2 = H$ **L2**, $R_1 = H$, $R_2 = OC_{18}H_{37}$

L3, $R_1 = OC_{18}H_{37}$, $R_2 = H$ **L4**, $R_1 = R_2 = OC_{18}H_{37}$

1: $Re(CO)_3Cl$**L1** **5**: $[Ru(bpy)_2$**L1**$](PF_6)_2$

2: $Re(CO)_3Cl$**L2** **6**: $[Ru(bpy)_2$**L2**$](PF_6)_2$

3: $Re(CO)_3Cl$**L3** **7**: $[Ru(bpy)_2$**L3**$](PF_6)_2$

4: $Re(CO)_3Cl$**L4** **8**: $[Ru(bpy)_2$**L4**$](PF_6)_2$

Experimental Section

Materials and Reagents. $Re(CO)_5Cl$ (98%, Strem), 4-nitrobiphenyl (98%, Fluka), 1-bromooctadecane (97%, Lancaster), and tin(II) chloride dehydrate (98%, Acros) were used as received. Pyridine-2-carboxaldehyde (99%, Aldrich) was purified by distillation before use. 5-Hydroxy-2-pyridinecarboxaldehyde,[13] 5-octadecyloxy-2-pyridinecarboxaldehyde,[14] 4-hydroxy-4′-nitrobiphenyl,[15] 4-aminobiphenyl,[16] 4-octadecyloxy-4′-aminobiphenyl,[16] and *cis*-$[Ru(bpy)_2Cl_2]$[17] were prepared according to literature methods. All solvents for synthesis were of analytical grade and were used without further purification.

Ligand Synthesis. The synthetic routes for the ligands are shown in Scheme 1.

***N*-(4-Biphenyl)pyridine-2-carbaldimine (L1). L1** was synthesized by modification of a literature method for the related pyridine-2-carbaldimines[18] by the condensation of pyridine-2-carboxaldehyde (0.21 g, 2.0 mmol) with 4-aminobiphenyl (0.34 g, 2.0 mmol) in refluxing ethanol (30 mL) in the presence of a catalytic amount of glacial acetic acid (0.5 mL) for 12 h. After cooling, the reaction mixture was reduced in volume under reduced pressure, and the residue was purified by column chromatography (EtOAc−hexanes, 1:5, v/v) on silica gel (230−400 mesh ASTM) to give the product as a pale yellow solid after removal of the solvents. Yield: 0.46 g, 90%. ^{1}H NMR (300 MHz, $CDCl_3$): δ 8.72 (d, 1H, $J = 4.3$ Hz), 8.68 (s, 1H), 8.23 (d, 1H, $J = 7.9$ Hz), 7.83 (m, 1H), 7.64 (m, 4H), 7.42 (m, 6H). EI-MS: *m*/*z* 258 $[M]^+$. Anal. Calcd for $C_{18}H_{14}N_2$: C, 83.70; H, 5.46; N, 10.84. Found: C, 83.86; H, 5.26; N, 10.68.

***N*-[4-(4′-Octadecyloxy)biphenyl]pyridine-2-carbaldimine (L2). L2** was synthesized as described for **L1** except that 4-octadecyloxy-4′-aminobiphenyl (0.88 g, 2.0 mmol) was used instead of 4-aminobiphenyl. Yield: 0.91 g, 86%. ^{1}H NMR (300 MHz, $CDCl_3$): δ 8.81 (d, 1H, $J = 4.0$ Hz), 8.73 (s, 1H), 8.22 (d, 1H, $J = 8.0$ Hz), 7.85 (m, 1H), 7.74 (d, 2H, $J = 6.1$ Hz), 7.67 (d, 2H, $J = 8.5$ Hz), 7.38 (m, 3H), 6.74 (d, 2H, $J = 8.5$ Hz), 4.00 (t, 2H, $J = 6.6$ Hz), 1.85 (m, 2H), 1.46 (m, 2H), 1.28 (m, 28H), 0.88 (t, 3H, $J = 6.6$ Hz). EI-MS: *m*/*z* 527 $[M]^+$. Anal. Calcd for $C_{36}H_{50}N_2O$: C, 82.08; H, 9.57; N, 5.32. Found: C, 81.86; H, 9.72; N, 5.26.

(5-Octadecyloxy)-2-pyridine-*N*-(4-biphenyl)carbaldimine (L3). L3 was synthesized as described for **L1** except that 5-octadecyloxy-2-pyridinecarboxaldehyde (0.75 g, 2.0 mmol) was used instead of pyridine-2-carboxaldehyde. Yield: 0.90 g, 86%. ^{1}H NMR (300 MHz, CD_2Cl_2): δ 8.65 (s, 1H), 8.36 (s, 1H), 8.17 (d, 1H, $J = 8.6$ Hz), 7.64 (m, 4H), 7.45 (m, 2H), 7.34 (m, 4H), 4.08 (t, 2H, $J = 6.6$ Hz), 1.82 (m, 2H), 1.48 (m, 2H), 1.28 (m, 28H), 0.88 (t, 3H, $J = 6.6$ Hz). EI-MS: *m*/*z* 526 $[M]^+$. Anal. Calcd for $C_{36}H_{50}N_2O$: C, 82.08; H, 9.57; N, 5.32. Found: C, 81.92; H, 9.65; N, 5.28.

(5-Octadecyloxy)-2-pyridine-*N*-[4-(4′-octadecyloxy)biphenyl]-carbaldimine (L4). L4 was synthesized as described for **L1** except that 5-octadecyloxy-2-pyridinearboxaldehyde (0.75 g, 2.0 mmol) and 4-octadecyloxy-4′-aminobiphenyl (0.88 g, 2.0 mmol) were used instead of pyridine-2-carboxaldehyde and 4-aminobiphenyl. Yield: 1.2 g, 75%. ^{1}H NMR (300 MHz, CD_2Cl_2): δ 8.59 (s, 1H), 8.36 (s, 1H), 8.17 (d, 1H, $J = 8.9$ Hz), 7.61 (d, 2H, $J = 8.6$ Hz), 7.56 (d, 2H, $J = 8.6$ Hz), 7.32 (m, 3H), 6.97 (d, 2H, $J = 8.7$ Hz), 4.08 (t, 2H, $J = 6.5$ Hz), 4.00 (t, 2H, $J = 6.6$ Hz), 1.82 (m, 4H), 1.48 (m, 4H), 1.28 (m, 56H), 0.88 (m, 6H). Positive FAB-MS: *m*/*z* 795 $[M]^+$. Anal. Calcd. for $C_{54}H_{86}N_2O_2$: C, 81.56; H, 10.90; N, 3.52. Found: C, 81.80; H, 11.12; N, 3.28.

Syntheses of Rhenium(I) Diimine Complexes *fac*-$[Re(CO)_3ClL]$. The complexes were synthesized by modification of a literature procedure for related complexes.[19] A mixture of $Re(CO)_5Cl$ (54.3 mg, 0.15 mmol) and L (0.15 mmol) in benzene (30 mL) was heated to reflux under N_2 for 4 h. After removal of the solvent, the residue was recrystallized three times from CH_2Cl_2−hexane to afford the product. Slow diffusion of diethyl ether vapor into a CH_2Cl_2 solution of *fac*-$[ClRe(CO)_3L]$ afforded the desired complex.

$[Re(CO)_3ClL1]$ (1): yellow crystals, yield 74 mg, 88%. ^{1}H NMR (400 MHz, $CDCl_3$): δ 9.11 (d, 1H, $J = 5.3$ Hz), 8.84 (s, 1H), 8.08 (m, 2H), 7.73 (dd, 2H, $J_1 = 6.6$ Hz, $J_2 = 2.0$ Hz), 7.62 (m, 4H), 7.43 (m, 4H). IR (Nujol, ν/cm^{-1}): 2023 (s) ν(CO), 1928 (vs) ν-(CO), 1895 (vs) ν(CO). Positive FAB-MS: *m*/*z* 564 $[M]^+$, 529 $[M - Cl]^+$. Anal. Calcd for $C_{21}H_{14}N_2O_3ClRe$: C, 44.72; H, 2.50; N, 4.97. Found: C, 44.61; H, 2.55; N, 4.82.

$[Re(CO)_3ClL2]$ (2): yellow powder, yield 107 mg, 86%. ^{1}H NMR (300 MHz, $CDCl_3$): δ 9.11 (d, 1H, $J = 5.3$ Hz), 8.83 (s, 1H), 8.12 (m, 1H), 8.04 (m, 1H), 7.62 (m, 7H), 7.00 (d, 2H, $J = 8.8$ Hz), 4.00 (t, 2H, $J = 6.6$ Hz), 1.85 (m, 2H), 1.47 (m, 2H), 1.26 (m, 28H), 0.88 (t, 3H, $J = 6.6$ Hz). IR (Nujol, ν/cm^{-1}): 2015 (s) ν(CO), 1935 (s) ν(CO), 1892 (s) ν(CO). Positive FAB-MS: *m*/*z* 832 $[M]^+$, 797 $[M - Cl]^+$. Anal. Calcd for $C_{39}H_{50}N_2O_4ClRe$: C, 56.27; H, 6.05; N, 3.37. Found: C, 56.20; H, 6.03; N, 3.18.

$[Re(CO)_3ClL3]$ (3): yellow crystals, yield 106 mg, 85%. ^{1}H NMR (400 MHz, $CDCl_3$): δ 8.72 (d, 1H, $J = 2.5$ Hz), 8.69 (s, 1H), 7.91(d, 1H, $J = 8.6$ Hz), 7.68 (d, 2H, $J = 8.6$ Hz), 7.61 (m, 2H), 7.55 (d, 2H, $J = 8.4$ Hz), 7.41 (m, 4H), 4.12 (t, 2H, $J = 6.5$ Hz), 1.87 (m, 2H), 1.48 (m, 2H), 1.26 (m, 28H), 0.88 (t, 3H, $J = 6.6$ Hz). IR (Nujol, ν/cm^{-1}): 2018 (s) ν(CO), 1911 (s) ν(CO), 1895 (s) ν(CO). Positive FAB-MS: *m*/*z* 832 $[M]^+$, 797 $[M - Cl]^+$. Anal. Calcd for $C_{39}H_{50}N_2O_4ClRe$: C, 56.27; H, 6.05; N, 3.37. Found: C, 56.38; H, 6.11; N, 3.54.

$[Re(CO)_3ClL4]$ (4): yellow powder, yield 138 mg, 84%. ^{1}H NMR (400 MHz, $CDCl_3$): δ 8.74 (d, 1H, $J = 2.5$ Hz), 8.69 (s, 1H), 7.90 (d, 1H, $J = 8.6$ Hz), 7.63 (d, 2H, $J = 8.6$ Hz), 7.53 (m, 4H), 7.41 (dd, 1H, $J_1 = 8.8$ Hz, $J_2 = 2.6$ Hz), 6.98 (d, 2H, $J = 8.7$ Hz), 4.13 (m, 2H), 4.00 (t, 2H, $J = 6.6$ Hz), 1.83 (m, 4H), 1.45 (m, 4H), 1.28 (m, 56H), 0.89 (m, 6H). IR (Nujol, ν/cm^{-1}): 2019 (s) ν(CO), 1921 (s) ν(CO), 1895 (s) ν(CO). Positive FAB-MS: *m*/*z* 1099 $[M^+]$, 1064 $[M - Cl]^+$. Anal. Calcd for $C_{57}H_{86}N_2O_5ClRe$: C, 62.18; H, 7.87; N, 2.54. Found: C, 62.45; H, 7.98; N, 2.64.

Syntheses of Ruthenium(II) Bipyridyl Complexes $[Ru(bpy)_2L](PF_6)_2$. The complexes were synthesized by modification of a

(13) Hass, W.; Koenig, W. A. *Liebigs Ann. Chem.* **1982**, *9*, 1615.
(14) Zhang, J. X. Ph.D. Thesis, The University of Hong Kong.
(15) Hajduk, P. J.; Sheppard, G.; Nettesheim, D. G.; Fesik, S. W. *J. Am. Chem. Soc.* **1997**, *119*, 5818.
(16) (a) Liu, X. H.; Abser, N.; Bruce, D. W. *J. Organomet. Chem.* **1998**, *551*, 271. (b) Coe, B. J.; Jones, C. J.; McCleverty, J. A.; Bruce, D. W. *Polyhedron* **1993**, *12*, 45.
(17) Sullivan, B. P.; Salmon, D. J.; Meyer, T. J. *Inorg. Chem.* **1978**, *17*, 3334.
(18) Johnson, D. W.; Mayer, H. K.; Minard, J. P.; Banatida, J.; Miller, C. *Inorg. Chim. Acta* **1988**, *144*, 167.
(19) Wrighton, M. S.; Morse, D. L. *J. Am. Chem. Soc.* **1974**, *96*, 998.

literature procedure for related complexes.[12d] A mixture of of *cis*-$[Ru(bpy)_2Cl_2]$ (52 mg, 0.1 mmol) and L (0.11 mmol) in absolute ethanol (30 mL) was heated to reflux for 12 h. After cooling to room temperature, the solution was filtered and the filtrate was reduced in volume. A saturated solution of NH_4PF_6 in methanol was added. The desired product was obtained by filtration and recrystallization by vapor diffusion of diethyl ether into a CH_2Cl_2 solution of the complex.

$[Ru(bpy)_2L1](PF_6)_2$ (5): deep red crystals, yield 67 mg, 82%. ^{1}H NMR (400 MHz, acetone-d_6): δ 9.35 (s, 1H), 8.97 (d, 1H, J = 5.6 Hz), 8.87 (dd, 2H, J_1 = 8.0 Hz, J_2 = 4.4 Hz), 8.58 (m, 2H), 8.35−7.91 (m, 10H), 7.80−7.35 (m, 12H), 6.88 (d, 2H, J = 4.7 Hz). Positive FAB-MS: m/z 817 $[M - PF_6]^+$, 672 $[M - 2PF_6]^+$, 336 $[M - 2PF_6]^{2+}$. Anal. Calcd for $C_{38}H_{30}N_6P_2F_{12}Ru$: C, 47.46; H, 3.14; N, 8.74. Found: C, 47.43; H, 3.22; N, 8.50.

$[Ru(bpy)_2L2](PF_6)_2$ (6): brown powder, yield 87 mg, 80%. ^{1}H NMR (400 MHz, acetone-d_6): δ 9.46 (s, 1H), 8.95 (d, 1H, J = 5.6 Hz), 8.87 (t, 2H, J = 7.1 Hz), 8.58 (m, 2H), 8.36−7.94 (m, 10H), 7.77−7.66 (m, 3H), 7.58 (m, 1H), 7.44 (m, 3H), 7.32 (d, 2H, J = 8.5 Hz), 6.98 (d, 2H, J = 8.7 Hz), 6.85 (d, 2H, J = 8.5 Hz), 4.03 (t, 2H, J = 6.6 Hz), 1.80 (m, 2H), 1.45 (m, 2H), 1.28 (m, 28H), 0.87 (t, 3H, J = 6.6 Hz). Positive FAB-MS: m/z 1085 $[M - PF_6]^+$, 940 $[M - 2PF_6]^+$, 470 $[M - 2PF_6]^{2+}$. Anal. Calcd for $C_{56}H_{66}N_6OP_2F_{12}Ru$: C, 54.68; H, 5.41; N, 6.83. Found: C, 54.76; H, 5.32; N, 6.92.

$[Ru(bpy)_2L3](PF_6)_2$ (7): brown powder, yield 87 mg, 80%. ^{1}H NMR (400 MHz, acetone-d_6): δ 9.30 (s, 1H), 8.98 (d, 1H, J = 5.8 Hz), 8.84 (t, 2H, J = 7.5 Hz), 8.54 (m, 2H), 8.34−8.13 (m, 6H), 7.95−7.66 (m, 6H), 7.57−7.32 (m, 9H), 6.82 (d, 2H, J = 4.8 Hz), 4.11 (t, 2H, J = 6.6 Hz), 1.70 (m, 2H), 1.28 (m, 30H), 0.87 (t, 3H, J = 6.6 Hz). Positive FAB-MS: m/z 1085 $[M - PF_6]^+$, 940 $[M - 2PF_6]^+$, 470 $[M - 2PF_6]^{2+}$. Anal. Calcd for $C_{56}H_{66}N_6OP_2F_{12}Ru$: C, 54.68; H, 5.41; N, 6.83. Found: C, 54.86; H, 5.53; N, 6.95.

$[Ru(bpy)_2L4](PF_6)_2$ (8): brown powder, yield 106 mg, 78%. ^{1}H NMR (400 MHz, acetone-d_6): δ 9.28 (s, 1H), 8.96 (d, 1H, J = 5.6 Hz), 8.86 (t, 2H, J = 8.9 Hz), 8.53 (m, 2H), 8.33−8.12 (m, 6H), 7.94−7.66 (m, 6H), 7.56 (m, 1H), 7.41 (m, 3H), 7.28 (dd, 2H, J_1 = 6.7 Hz, J_2 = 1.9 Hz), 6.96 (dd, 2H, J_1 = 6.8 Hz, J_2 = 2.0 Hz), 6.78 (dd, 2H, J_1 = 6.7, Hz, J_2 = 1.9 Hz), 4.10 (t, 2H, J = 6.6 Hz), 4.01 (t, 2H, J = 6.5 Hz), 1.74 (m, 4H), 1.47 (m, 4H), 1.28 (m, 56H), 0.87 (m, 6H). Positive FAB-MS: m/z 1354 $[M - PF_6]^+$, 1209 $[M - 2PF_6]^+$, 605 $[M - 2PF_6]^{2+}$. Anal. Calcd for $C_{74}H_{102}N_6O_2P_2F_{12}Ru$: C, 59.31; H, 6.86; N, 5.61. Found: C, 59.56; H, 6.75; N, 5.46.

Physical Measurements and Instrumentation. All electronic absorption spectra were recorded on a Hewlett-Packard 8452A diode array spectrophotometer. ^{1}H NMR spectra were recorded on a Bruker DPX-300 (300 MHz) or Bruker DPX-400 (400 MHz) FT-NMR spectrometer. Chemical shifts were reported relative to Me_4Si. Elemental analyses were performed by the Institute of Chemistry at the Chinese Academy of Sciences in Beijing. All EI and positive-ion FAB mass spectra were recorded on a Finnigan MAT95 mass spectrometer. IR spectra were obtained as Nujol mulls on a Bio-Rad FTS-7 IR spectrometer. Steady-state emission and excitation spectra recorded at room temperature were obtained on a Spex Fluorolog-2 model F111 fluorescence spectrophotometer. All solutions for photophysical studies were prepared under high vacuum in a 10 cm^3 round-bottomed flask equipped with a sidearm 1 cm fluorescence cuvette and sealed from the atmosphere by a Rotaflo HP6/6 quick-release Teflon stopper. Solutions were rigorously degassed with no fewer than four successive freeze−pump−thaw cycles.

Emission lifetime measurements were performed using a conventional laser system. The excitation source was the 355 nm output (third harmonic) of a Spectra-Physics Quanta-Ray Q-switched GCR-150-10 pulsed Nd:YAG laser. Luminescence decay signals from a Hamamatsu R928 photomultiplier tube were converted to voltage changes by connecting to a 50 Ω load resistor and were then recorded on a Tektronix model TDS 620A digital oscilloscope. The lifetime τ was determined by a single-exponential fitting of the luminescence decay traces with the model $I(t) = I_0 \exp(-t/\tau)$, where $I(t)$ and I_0 stand for the luminescence intensity at time = t and time = 0, respectively. Solution samples for luminescence lifetime measurements were degassed with no fewer than four successive freeze−pump−thaw cycles.

Langmuir−Blodgett (LB) Film Preparation. Ultrapure water (resistance >18 MΩ cm) was obtained from an Elga UHQ PS system and was immediately used for the Z-type LB film preparation. The quartz substrates were made hydrophilic by consecutive sonication in detergent for 30 min and acetone for 15 min and soaking in both chromic acid and piranha solution (30% H_2O_2−H_2SO_4, 3:7 v/v) for 8 h each before they were finally washed repeatedly with copious amounts of distilled and ultrapure water. The complexes in dichloromethane with concentration of ca. 1 mg cm^{-3} were spread onto a pure water phase (pH 5.4, 18 °C) in a Nima model-622 computer-controlled Langmuir−Blodgett trough. After a 15 min period to allow for the evaporation of the solvent, surface pressure−area (π−A) isotherms were recorded at a barrier compression speed of 150 cm^2 min^{-1}. The monolayers formed under a constant surface pressure were transferred onto hydrophilically treated quartz substrates after maintaining the pressure constant at the transfer pressure for 15 min for stabilization, at a dipping speed of 5 mm min^{-1}. The transfer ratios were close to unity.

Second-Harmonic Generation (SHG) Measurements. The setup for SHG measurements was similar to that reported in the literature.[12d,20] The experimental measurements were made in transmission geometry using a Y-cut quartz crystal as reference. The source was the fundamental 1064 nm output of a Spectra-Physics Quanta-Ray Q-switched GCR-150-10 pulsed Nd:YAG laser. A half-wave plate and a Glan-Taylor polarizer were used to vary the polarization direction of the laser beam. The fundamental light, linearly polarized either parallel (p) or perpendicular (s) to the plane of incidence, was focused by a quartz lens (50 mm focal length) and was directed at an incident angle of 45° onto the vertically mounted sample. Before the laser beam passed through the film, a dichroic process filter was used to filter off the 532 nm signal generated by the optical lens. The 532 nm signals generated were recorded on a Tektronix TDS-620A digital oscilloscope. Prior to each measurement, the monolayer film at the back side of the substrate was wiped off carefully with lens tissue soaked with chloroform in order to prevent interference between signals arising from the monolayers at the front and back side of the substrate. The SHG data were analyzed by the general procedure described by Ashwell et al.[21]

Crystal Structure Determination. Slow diffusion of diethyl ether vapor into the respective dichloromethane solutions of complexes **1** and **5** afforded diffraction-quality crystals of **1** and **5**.

A yellow crystal of **1** of dimensions 0.5 mm × 0.15 mm × 0.1 mm mounted in a glass capillary was used for data collection at −20 °C on a MAR diffractometer with a 300 mm image plate detector using graphite-monochromatized Mo Kα radiation (λ = 0.71073 Å). Data collection was made with 3° oscillation steps of φ, 300 s exposure time, and scanner distance at 120 mm. Forty images were collected. The images were interpreted and intensities integrated using the program DENZO.[22] The structure was solved by direct methods employing the SIR-97[23] program on a PC. Re, Cl, and most of the non-hydrogen atoms were located according to the direct methods and the successive least-squares Fourier cycles.

(20) (a) Dougherty, J. P.; Kurtz, S. K. *J. Appl. Crystallogr.* **1976**, *9*, 145. (b) Girling, I. R.; Cade, N. A.; Kolinsky, P. V.; Peterson, I. R.; Ahmad, M. M.; Neal, D. B.; Petty, M. C.; Roberts, G. G.; Feast, W. J. *J. Opt. Soc. Am.* **1987**, *B4*, 950.

(21) Ashwell, G. J.; Hargreaves, R. C.; Baldwin, C. E.; Bahra, G. S.; Brown, C. R. *Nature* **1992**, *357*, 393.

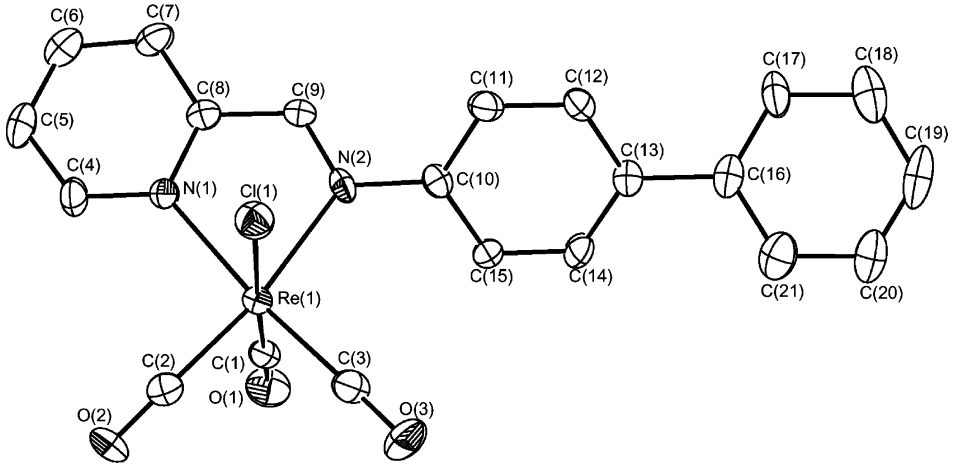

Figure 1. Perspective drawing of complex **1** with atomic numbering scheme. Hydrogen atoms have been omitted for clarity. Thermal ellipsoids are shown at the 30% probability level.

Positions of other non-hydrogen atoms were found after successful refinement by full-matrix least-squares using the program SHELXL-97[24] on a PC. According to the SHELXL-97[24] program, all 3383 independent reflections from a total 6854 reflections were used in the full-matrix least-squares refinement against F^2. These reflections were in the range $-9 \le h \le 9$, $-14 \le k \le 20$, $-16 \le l \le 16$ with $2\theta_{max} = 51.26°$. A crystallographic asymmetric unit comprised one molecule. In the final stage of least-squares refinement, all non-hydrogen atoms of the molecule were refined anisotropically. Hydrogen atoms were generated by the program SHELXL-97.[24] The positions of hydrogen atoms were calculated on the basis of the riding mode with thermal parameters equal to 1.2 times that of the attached carbon atoms and were used in the calculation of final *R* indices. Convergence for 253 variable parameters by full-matrix least-squares refinement against F^2 reached $R_1 = 0.0379$ and $wR_2 = 0.0947$ with a goodness-of-fit of 0.979; the parameters *a* and *b* for the weighting scheme are 0.0395 and 0. The final difference Fourier map showed maximum rest peaks and holes of 1.294 and -1.407 e Å^{-3}, respectively. The crystal and structure determination data of **1** are summarized in Table S1.

A deep red crystal of **5** of dimensions 0.5 mm × 0.15 mm × 0.08 mm mounted in a glass capillary was used for data collection at −20 °C on a MAR diffractometer with a 300 mm image plate detector using graphite-monochromatized Mo Kα radiation (λ = 0.71073 Å). Data collection was made with 2° oscillation steps of φ, 600 s exposure time, and scanner distance at 120 mm. Ninety images were collected. The images were interpreted and intensities integrated using the program DENZO.[22] The structure was solved by direct methods employing the SIR-97[23] program on a PC. Ru, P, and many non-hydrogen atoms were located according to the direct methods and the successive least-squares Fourier cycles. Positions of other non-hydrogen atoms were found after successful refinement by full-matrix least-squares using the program SHELXL-97[24] on a PC. Two PF_6 anions were located. According to the SHELXL-97[24] program, all 3705 independent reflections from a total 9808 reflections were used in the full-matrix least-squares refinement against F^2. These reflections were in the range $-8 \le h \le 9$, $-34 \le k \le 36$, $-11 \le l \le 14$ with $2\theta_{max} = 48.90°$. One crystallographic asymmetric unit consisted of one formula unit. In the final stage of least-squares refinement, all non-hydrogen atoms of the molecule were refined anisotropically. Hydrogen atoms were generated by the program SHELXL-97.[24] The positions of H atoms were calculated on the basis of the riding mode with thermal parameters equal to 1.2 times that of the associated carbon atoms and were used in the calculation of final *R* indices. Convergence for 532 variable parameters by full-matrix least-squares refinement on F^2 reached $R_1 = 0.0405$ and $wR_2 = 0.0874$ with a goodness-of-fit of 0.835; the parameters *a* and *b* for the weighting scheme are 0.0 and 0. The final difference Fourier map showed maximum rest peaks and holes of 0.356 and -0.315 e Å^{-3}, respectively. The crystal and structure determination data of **5** are summarized in Table S2.

Table 1. Selected Bond Distances (Å) and Bond Angles (deg) for Complex 1

	Distances		
Re−Cl(1)	2.467(2)	Re−N(1)	2.173(6)
Re−N(2)	2.182(6)	Re−C(1)	1.915(9)
Re−C(2)	1.907(9)	Re−C(3)	1.929(10)
C(8)−N(1)	1.347(9)	C(9)−N(2)	1.298(10)
C(1)−O(1)	1.097(9)	C(2)−O(2)	1.148(9)
C(3)−O(3)	1.131(1)		
	Angles		
Cl(1)−Re−N(1)	84.38(15)	Cl(1)−Re−N(2)	82.88(15)
Cl(1)−Re−C(1)	177.3(2)	Cl(1)−Re−C(2)	93.6(2)
Cl(1)−Re−C(3)	91.50(2)	N(1)−Re−N(2)	74.8(2)
N(1)−Re−C(1)	96.0(3)	N(1)−Re−C(2)	96.4(3)
N(1)−Re−C(3)	173.6(3)	N(2)−Re−C(1)	94.6(3)
N(2)−Re−C(2)	170.8(2)	N(2)−Re−C(3)	99.8(3)
C(1)−Re−C(2)	89.0(3)	C(1)−Re−C(3)	87.9(3)
C(2)−Re−C(3)	88.7(4)	C(9)− N(2)−C(10)	117.2(7)
Re−N(2)−C(9)	115.5(6)	Re−N(2)−C(10)	127.0(5)

Results and Discussion

Syntheses and Characterization. The Ru(II) and Re(I) complexes were prepared in good yields according to modification of literature methods.[12d,19] All of the newly synthesized complexes gave satisfactory elemental analyses and were characterized by UV−vis spectroscopy, positive FAB-MS, IR, and ^{1}H NMR spectroscopy. The IR spectra of the Re(I) complexes show three intense absorption bands in the region 1860−2040 cm^{-1}, typical of the facial arrangement of the three carbonyl groups.[25] The structures of complexes **1** and **5** were also determined by X-ray crystallography.

(22) Otwinowski, Z.; Minor, W. In *Processing of X-ray Diffraction Data Collected in Oscillation Mode, Methods in Enzymology, Vol. 276: Macromolecular Crystallography*; Carter, C. W., Sweet, R. M., Jr., Eds.; Academic Press: New York, 1997; pp 307−326. .

(23) Altomare, A.; Burla, M. C.; Camalli, M.; Cascarano, G.; Giacovazzo, C.; Guagliardi, A.; Moliterni, A. G. G.; Polidori, G.; Spagna, R. *Sir97*: a new tool for crystal structure determination and refinement. *J. Appl. Crystallogr.* **1998**, *32*, 115.

(24) SHELXL97: Sheldrick, G. M. *SHELX97*, Programs for Crystal Structure Analysis (Release 97-2); University of Goetingen: Germany, 1997.

(25) Giordano, P. J.; Wrighton, M. S. *J. Am. Chem. Soc.* **1979**, *101*, 2888.

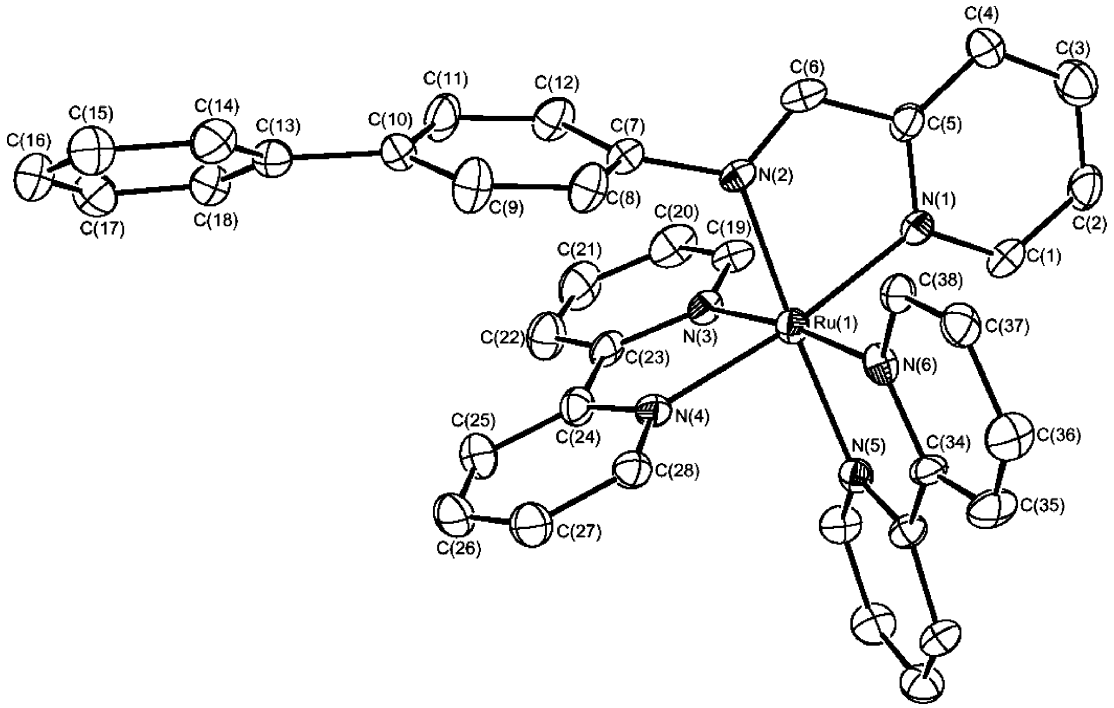

Figure 2. Perspective drawing of the complex cation of **5** with atomic numbering scheme. Hydrogen atoms have been omitted for clarity. Thermal ellipsoids are shown at the 30% probability level.

Table 2. Selected Bond Distances (Å) and Angles (deg) for Complex 5

	Distances		
Ru(1)−N(1)	2.066(4)	Ru(1)−N(2)	2.035(4)
Ru(1)−N(3)	2.060(4)	Ru(1)−N(4)	2.060(4)
Ru(1)−N(5)	2.081(5)	Ru(1)−N(6)	2.068(4)
N(2)−C(6)	1.297(6)	N(2)−C(7)	1.450(6)
C(5)−C(6)	1.436(7)	C(10)−C(13)	1.502(7)
	Angles		
N(1)−Ru(1)−N(2)	77.54(18)	N(1)−Ru(1)−N(3)	97.09(18)
N(1)−Ru(1)−N(4)	173.12(19)	N(1)−Ru(1)−N(5)	100.78(18)
N(1)−Ru(1)−N(6)	88.23(15)	N(2)−Ru(1)−N(3)	86.71(16)
N(2)−Ru(1)−N(4)	96.64(17)	N(2)−Ru(1)−N(5)	175.6(2)
N(2)−Ru(1)−N(6)	97.8(2)	N(3)−Ru(1)−N(4)	78.8(2)
N(3)−Ru(1)−N(5)	97.3(3)	N(3)−Ru(1)−N(6)	173.67(19)
N(4)−Ru(1)−N(5)	85.29(15)	N(4)−Ru(1)−N(6)	96.27(18)
N(5)−Ru(1)−N(6)	78.0(2)	C(6)−N(2)−C(7)	121.3(4)

Table 3. Electronic Absorption and Emission Properties of Complexes 1−8 at 298 K

complex	medium	absorption λ/nm ($\epsilon \times 10^{-4}$/dm^3 mol^{-1} cm^{-1})	emission[a] λ/nm (τ_o/μs)
1	CH_2Cl_2	256 (3.43), 364 (1.32)	789 (<0.1)
2	CH_2Cl_2	272 (3.33), 398 (1.00)	785 (<0.1)
3	CH_2Cl_2	256 (3.20), 302 (1.72), 356 (1.97)	757 (<0.1)
4	CH_2Cl_2	262 (2.83), 307 sh (1.40), 382 (1.58)	756 (<0.1)
5	CH_3CN	256 sh (3.82), 286 (6.23), 344 sh (1.56), 426 (0.96), 486 (0.96)	798 (<0.1)
6	CH_3CN	256 (3.12), 286 (7.26), 342 (1.53), 370 (1.48), 422 (1.33), 478 (1.09)	796 (<0.1)
7	CH_3CN	256 (3.38), 288 (6.86), 342 sh (2.17), 422 sh (1.01), 456 (1.28), 470 (1.18)	773 (<0.1)
8	CH_3CN	256 (3.36), 288 (8.74), 344 (2.00), 370 sh (1.74), 456 (1.25), 472 (1.10)	772 (<0.1)

[a] Corrected for PMT response.

Crystal Structure. A perspective drawing of complex **1** with atomic numbering is shown in Figure 1. The coordination geometry at the Re atom is distorted octahedral with the three carbonyl ligands arranged in a facial fashion, which is in agreement with the result observed from IR data. Selected bond distances and angles for complex **1** are given in Table 1. The N(1)−Re−N(2) bond angle of 74.8° (less than 90°) is a result of the steric requirement of the bidentate diimine ligand. All other bond distances and bond angles are comparable to those found for the related rhenium(I) polypyridyl complexes.[9a,11b,26] The dihedral angle between the planes of the pyridine-containing diimine ligand and the adjacent phenyl ring is 40.12°, and that within the biphenyl rings is 24.90°.

A perspective drawing of the complex cation of **5** is shown in Figure 2, and selected bond distances and angles are given in Table 2. The coordination geometry at the Ru atom is also distorted octahedral. The N−Ru−N bond angles subtended by the chelating bipyridine ligands are 78.0(2)° to 78.8(2)° and that by the diimine ligand is 77.54(18)°. The deviation from the ideal 90° for a regular octahedral geometry is a result of the steric requirement of the bidentate ligands. The dihedral angle between the planes of the pyridine-containing diimine ligand and the adjacent phenyl ring is 78.91°, and that within the biphenyl rings is 33.55°. It is expected that conjugation between the biphenyl unit and the chelating diimine ligand is small.

Electronic Absorption Spectroscopy. The electronic absorption and emission spectral data for all the complexes are summarized in Table 3. For the rhenium complexes **1**−**4**, their UV−vis absorption spectra display very intense absorptions in the 256−307 nm region and less intense absorption bands at ca. 356−398 nm in dichloromethane at 298 K. The high-energy absorptions, which also occur in the free ligands, are ascribed to the intraligand (IL) $\pi \rightarrow \pi^*$ transitions, and the low-energy absorption bands are most likely derived from an admixture of dπ(Re) $\rightarrow \pi^*$(diimine) metal-to-ligand charge transfer (MLCT) and IL $\pi \rightarrow \pi^*$ transitions, in view of the high extinction coefficients ($\sim 10^4$ dm^3 mol^{-1} cm^{-1}) and the presence of low-energy components in the same region for the free ligands. The ruthenium(II) complexes **5**−**8** show very intense absorption

(26) (a) Yam, V. W. W.; Lau, V. C. Y.; Cheung, K. K. *J. Chem. Soc., Chem. Commun.* **1995**, *259*, 1195. (b) Yam, V. W. W.; Lo, K. K. W.; Cheung, K. K.; Kong, R. Y. C. *J. Chem. Soc., Chem. Commun.* **1995**, *259*, 1191. (c) Lees, A. J. *Comm. Inorg. Chem.* **1995**, *17*, 319.

Table 4. LB Film-Forming Properties of Re(I) and Ru(II) Complexes

complex	molecular area/Å^2	collapse pressure /mN m^{-1}
2	53	>55
3	52	7
6	77	>40
7	113	>30
8	145	>18

bands at ca. 236−344 nm with a shoulder at ca. 370 nm and low-energy absorption bands at ca. 426−456 nm and 470−486 nm in acetonitrile at 298 K. The absorption bands at ca. 236−344 nm are assigned to intraligand (IL) $\pi \rightarrow \pi^*$ transitions, while the shoulders at ca. 370 nm are originated from the low-energy components of IL bands. With reference to previous spectroscopic studies on related ruthenium(II) complexes possessing diimine ligands,[12d,27] the bands at ca. 426−456 nm are assigned to an admixture of the $\pi \rightarrow \pi^*$ IL and dπ(Ru) $\rightarrow \pi^*$-(bpy) MLCT transitions, while the bands at ca. 470−486 nm are assigned to the dπ(Ru) $\rightarrow \pi^*$(diimine) MLCT transitions. The higher MLCT absorption energies of complexes **7** (470 nm) and **8** (472 nm) than complexes **5** (486 nm) and **6** (478 nm) are in line with the presence of electron-donating alkoxy substituents on the pyridyl rings of the ligands in complexes **7** and **8**, which renders the ligands on complexes **7** and **8** more electron-rich and hence the π^*(L) orbital higher lying in energy. On the contrary, the alkoxy substituent on the biphenyl rings of the diimine ligand in complex **6** did not have any substantial effects on the absorption energies with reference to complex **5**. This is probably due to the poor π-conjugation and noncoplanarity of the biphenyl unit with the chelating diimine ligand, as revealed by the X-ray crystal structure determination.

Emission Spectroscopy. The emission spectra of complexes **1**−**8** show broad bands centered at ca. 756−798 nm (Table 3), and they are assigned to dπ(Re) or dπ(Ru) $\rightarrow \pi^*$(diimine) MLCT phosphorescence, respectively. Similar to that observed in the electronic absorption spectroscopy, the MLCT emission energies of complexes **1**−**8** are also found to depend on the position of electron-donating alkoxy substituent of the ligands. When compared to the pyridyl ring, the substituent on the biphenyl rings does not give rise to significant changes in the MLCT emission energy owing to the poor π-conjugation between the biphenyl unit and the chelating diimine ligand. Thus the emission energies of complexes **3** (757 nm) and **4** (756 nm) are higher than those of complexes **1** (789 nm) and **2** (785 nm). Similarly, blue shifts in emission energies of complexes **7** (773 nm) and **8** (772 nm) relative to complexes **5** (798 nm) and **6** (796 nm) are also observed. It is found that, with the same diimine ligand, the emission energy of the rhenium complex system is always higher than that of the ruthenium complex system. This is in line with the MLCT assignment, as the dπ-(Re) orbital of the rhenium(I) tricarbonyl diimine system is lower-lying in energy with reference to the dπ(Ru) orbital of the ruthenium(II) tris(diimine) system.

Surface Pressure−Area (π−*A*) Isotherm. The molecular areas and collapse pressures of the complexes are summarized in Table 4. Since complexes **1** and **5** lack hydrophobic moieties while complex **4** is too hydrophobic, the π−*A* isotherms of these three complexes cannot be recorded. Complex **2** displays good film-forming property with a well-defined transition in the π−*A* isotherm and high collapse pressure (Figure 3). It is interesting to note that complexes **2** and **3**, possessing the same hydrophilic heads (rhenium(I) centers) and the same hydrophobic tails (long hydrocarbon chains at different positions), have similar molecular areas of ca. 53 Å^2 per molecule, but substantially different collapse pressures. The collapse pressure of complex **3** (ca. 7 mN m^{-1}) is found to be much lower than that of complex **2** (ca. 55 mN m^{-1}), and no stable condensed monolayer for complex **3** at the air/water interface can be obtained due to its very low collapse pressure. It is proposed that the placement of the hydrophobic biphenyl rings and the long hydrocarbon tail at both ends of the hydrophilic head in complex **3** is unfavorable to the formation of stable thin films. From the π−*A* isotherm of complex **6**, a well-defined condensed region with collapse pressures of ca. 40 mN m^{-1} is observed (Figure 4), suggesting that it exhibits good and stable monolayer film-forming property. The molecular area of complex **8** (ca. 155 Å^2 per molecule) is found to be almost twice that of complex **6** (ca. 77 Å^2 per molecule), and this can be accounted for by the steric requirement of two hydrocarbon tails in the former complex as opposed to one in the latter. Aggregation of monolayers or multilayer structure formation is observed in the π−*A* isotherms of complexes **7** and **8** at higher surface pressures (Figure 4). This observation is indicative of their poorer film-forming properties

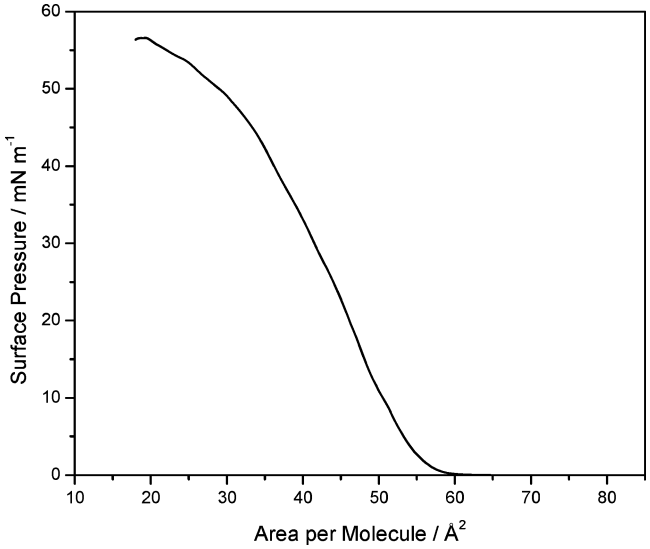

Figure 3. Surface pressure−area (π−*A*) isotherms of **2**.

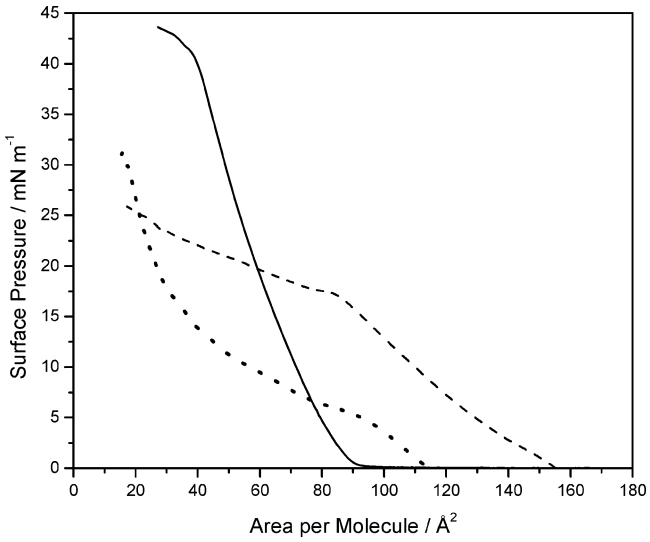

Figure 4. Surface pressure−area (π−*A*) isotherms of **6** (—), **7** (····), and **8** (---).

(27) (a) Brown, G. M.; Weaver, T. R.; Keene, F. R.; Meyer, T. J. *Inorg. Chem.* **1976**, *15*, 190. (b) Yam, V. W. W.; Lee, V. W. M. *J. Chem. Soc., Dalton Trans.* **1997**, 3005.

Table 5. Tilt Angles and First Molecular Hyperpolarizabilities of Complexes 2 and 6 in Langmuir−Blodgett Films

complex	molecular tilt angle ϕ/deg	first molecular hyperpolarizability β/esu	relative SHG intensity β/β (BI)[a]
2	29.5	2.79×10^{-28}	1.86
6	36.3	2.53×10^{-28}	1.69

[a] BI = (*E*)-*N*-methyl-4-(2-(4-octadecyloxyphenyl)ethenyl)pyridinium iodide.

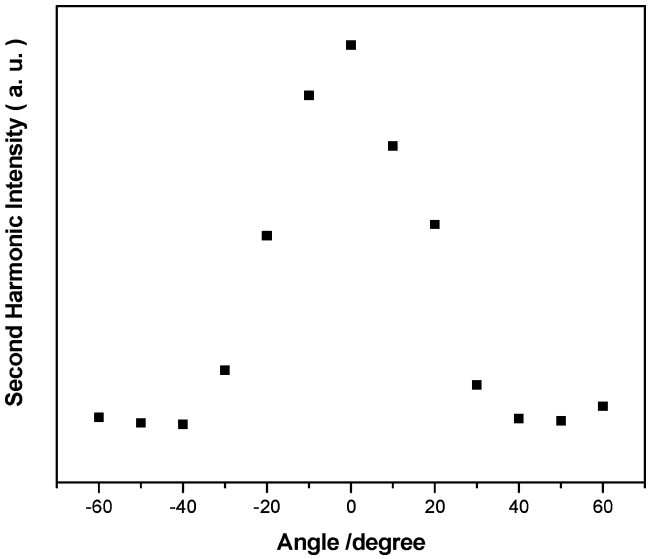

Figure 5. Normalized SHG intensity vs polarization angle from a monolayer film of complex **2**. The peaks and troughs correspond to the signal from p-polarized and s-polarized fundamental beams, respectively, while the abscissa corresponds to the angle of rotation of the half-wave plate.

and can probably be explained by the same reason as for complex **3**.

Second-Harmonic Generation (SHG) Properties. The SHG results are summarized in Table 5 and compared with that reported for the monolayer film of (*E*)-*N*-methyl-4-(2-(4-octadecyloxyphenyl)ethenyl)pyridinium iodide (BI, $\beta = 1.5 \times 10^{-28}$ esu).[28] The polarization dependence of the SHG from a monolayer of complex **2** is shown in Figure 5. The first-order hyperpolarizability β value of 2.79×10^{-28} esu for complex **2** is higher than that for the related complex *fac*-[ClRe(CO)$_3$L] (L = *N*-(4′-hexadecylphenyl)pyridine-2-carbaldimine, $\beta = 0.54 \times 10^{-28}$ esu).[11b] This agrees well with the fact that the SHG behavior of these metal complexes originates from their MLCT character.[7c,d,f] The increase in β value compared to related complexes is probably attributed to the structural difference between the LB films of these two complexes, in which a large difference in the molecular tilt angle (29.5° for complex **2** vs ca. 25° for related complexes) and different film-forming property as indicated from the $\pi-A$ isotherms of the complexes are observed. For complex **6**, a large β value of 2.53×10^{-28} esu, which is about 1.7 times that of the standard BI, is obtained. An electronic transition from the ruthenium(II) metal center to the diimine ligand is responsible for the large first-order hyperpolarizability of complex **6**. On the contrary, the monolayer films of complexes **3**, **7**, and **8** show only very weak SHG signals. The weak SHG behavior observed for these three complexes is most probably associated with the poor film-forming behavior of these complexes, which does not result in an ordered acentrosymmetric structure.

Conclusion

Several novel rhenium(I) and ruthenium(II) diimine complexes were synthesized and characterized. Their film formation properties, $\pi-A$ isotherms, and structures were discussed. Two of the complexes were capable of exhibiting relatively strong second-harmonic signals, which are in accordance with their good film-forming properties and their metal-to-ligand charge-transfer characteristics.

Acknowledgment. V.W.-W.Y. acknowledges financial support from the University Development Fund of The University of Hong Kong, and J.Z. acknowledges the receipt of a Postgraduate Studentship, administered by The University of Hong Kong.

Supporting Information Available: Tables detailing crystal data and refinement details for complex **1** and **5**, and their corresponding CIF files giving crystal data. These materials are available free of charge via the Internet at http://pubs.acs.org.

OM070030B

(28) Lupo, D.; Prass, W.; Scheunemann, U.; Laschewsky, A.; Ringsdorf, H.; Ledoux, I. *J. Opt. Soc. Am. B* **1988**, *5*, 300.